

## CATALYTIC STEAM REFORMING OF ETHANOL FOR HYDROGEN PRODUCTION OVER Ni/CeO<sub>2</sub>-ZrO<sub>2</sub> CATALYSTS

Zuogang Guo, Shurong Wang,\* Long Guo, and Xinbao Li

Ni/CeO<sub>2</sub>-ZrO<sub>2</sub> catalysts were prepared via co-precipitation and characterized by N<sub>2</sub> adsorption-desorption, XRD, SEM, and TPR techniques. The effects of reaction temperature, carbon-equivalent space velocity (G<sub>C1</sub>HSV), and steam-to-carbon ratio (S/C) on the performance of the catalysts for ethanol steam reforming (ESR) were investigated. It was found that the best catalytic performance was obtained over the Ni/Ce<sub>0.75</sub>Zr<sub>0.25</sub> catalyst with G<sub>C1</sub>HSV=345 h<sup>-1</sup> and S/C=9.2. Under these conditions, H<sub>2</sub> selectivity reached its highest value of 98% at T=725 °C, and carbon conversion reached 100% at T=825 °C. The performances of Ni/Ce<sub>0.75</sub>Zr<sub>0.25</sub> and Ni/Ce<sub>0.5</sub>Zr<sub>0.5</sub> were also compared at S/C ranging from 2.5 to 9.2. The results showed a higher carbon conversion for the Ni/Ce<sub>0.75</sub>Zr<sub>0.25</sub> catalyst than for Ni/Ce<sub>0.5</sub>Zr<sub>0.5</sub>.

*Keywords:* Steam Reforming; Hydrogen; Ethanol; Ni/CeO<sub>2</sub>-ZrO<sub>2</sub>; Biomass

*Contact information:* State Key Laboratory of Clean Energy Utilization, Zhejiang University, Hangzhou, 310027, P.R.China; \*Corresponding author: srwang@zju.edu.cn

### INTRODUCTION

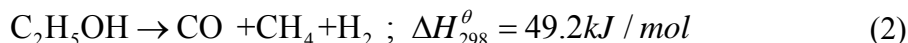
Current global energy consumption is mainly provided by fossil fuels and other non-renewable energy sources. The excessive consumption of fossil fuels leads to an increasing emission of greenhouse gases. With the gradual depletion of fossil fuel resources, biomass has attracted significant attention as a widely distributed, easily accessible, and renewable resource (Czernik et al. 2002). Hydrogen is an important energy resource and chemical raw material and is widely used in the hydrogenation of naphtha as well as in the metallurgical industry (Tsisun et al. 1981). Hydrogen also has potential application for the proton exchange membrane fuel cell (PEMFC). This is not restricted by the Carnot cycle, and can reach a high energy efficiency of up to 60% (Song 2005; Williams et al. 2004). However, traditional hydrogen production technology consumes large amounts of natural gas, oil, or coal (Luckow et al. 2010). The production of hydrogen from biomass has great potential when compared to fossil fuels (Wang et al. 1996). Since ethanol is one of the abundant compounds in biomass pyrolysis oil (bio-oil), research on ethanol reforming and its efficient catalysis is an important factor in bio-oil steam reforming.

Several reactions can occur during ethanol steam reforming (Chen et al. 2008), as described in Eqs. (1) - (4).

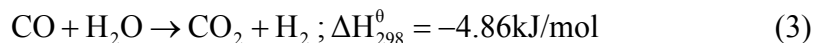
Ethanol steam reforming reaction (ESR):



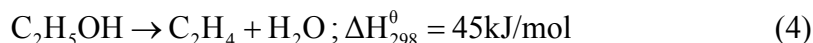
Ethanol decomposition reaction:



Water gas shift reaction (WGS):



Ethanol dehydration reaction:



The thermodynamic analysis of ethanol reforming carried out by Fishtik et al. (2000) indicates that steam reforming of ethanol does take place, and the yield of hydrogen can be increased by increasing the reaction temperature, as well as by controlling the process with a specified steam-to-carbon ratio and reaction pressure. In current studies, the catalysts used for ethanol reforming have mainly included noble metal based catalysts (Pt, Rh, Pd, and Ru), and non-noble metal catalysts (Ni, Cu, Co) (Breen et al. 2002). Liguras et al. (2003) studied the ethanol reforming reaction using Ru, Rh, and Pt catalysts supported on  $\text{Al}_2\text{O}_3$  and  $\text{MgO}$ . They found that a relatively low loading of Rh can lead to high catalytic activity, and the catalytic activity and hydrogen yield also increased to some extent with the increasing of metal loading amount. The hydrogen yield can reach over 90% with a 5% Rh/ $\gamma$ - $\text{Al}_2\text{O}_3$  catalyst. Silva et al. (2011) prepared Rh/ $\text{CeO}_2$  catalysts with different BET surface area, and they found that a higher BET surface area helped to increase the selectivity of acetaldehyde and eliminate carbon deposition. In contrast, a lower surface area promoted ethanol dehydration. However, because of the high cost of noble metal catalysts, Co, Cu, Ni, and other non-precious metal catalysts may have higher commercial values, and so these have attracted many researchers. Marino et al. (2003) studied the performance of Cu and Ni loaded on  $\gamma$ - $\text{Al}_2\text{O}_3$  in the steam reforming of ethanol and found that Cu mainly affected the cleavage of C-H and O-H bonds, and Ni was more responsible for C-C bond cleavage. Akande et al. (2005) conducted an ethanol reforming experiment over a Ni/ $\gamma$ - $\text{Al}_2\text{O}_3$  catalyst at different temperatures and Ni-loadings. Their studies indicated that strong interactions existed between the active sites and supports, and the crystal size had a great impact on the yield of hydrogen. Vargas et al. (2005) found that  $\text{CeO}_2$ , as a kind of support material for ethanol reforming, was not only conducive to the decomposition of ethanol and the water gas shift reaction, but also helped to improve the stability of the catalyst and increase the yield of hydrogen. It was also found that  $\text{ZrO}_2$  can adsorb  $\text{H}_2\text{O}$  to create supplementary surface hydroxyl groups for active sites.

In the present work, we prepared two kinds of Ni/ $\text{CeO}_2$ - $\text{ZrO}_2$  catalysts with different Ce/Zr ratios and applied them to the steam reforming of ethanol at different temperatures (T), steam-to-carbon ratios (S/C), and carbon-equivalent space velocities ( $G_{\text{C}_1\text{HSV}}$ ). We investigated the effects of these conditions on the hydrogen selectivity and carbon conversion.

## EXPERIMENTAL

### Catalyst Preparation

15 wt% Ni supported on CeO<sub>2</sub>-ZrO<sub>2</sub> catalysts were prepared by co-precipitation. Catalysts with different CeO<sub>2</sub>/ZrO<sub>2</sub> molar ratios: 0.75/0.25 and 0.5/0.5 were prepared. The two catalysts were denoted as Ni/Ce<sub>0.75</sub>Zr<sub>0.25</sub> and Ni/Ce<sub>0.5</sub>Zr<sub>0.5</sub>. For the preparation of Ni/Ce<sub>0.75</sub>Zr<sub>0.25</sub>, 7.43 g Ni(NO<sub>3</sub>)<sub>2</sub>•6H<sub>2</sub>O, 24 g Ce(NO<sub>3</sub>)<sub>3</sub>•6H<sub>2</sub>O, and 6.3 g Zr(NO<sub>3</sub>)<sub>4</sub>•5H<sub>2</sub>O were dissolved in deionized water and stirred at 40 °C in a water bath for 30 minutes to form solution A. For the preparation of the catalyst Ni/Ce<sub>0.5</sub>Zr<sub>0.5</sub>, 7.43 g Ni(NO<sub>3</sub>)<sub>2</sub>•6H<sub>2</sub>O, 16 g Ce(NO<sub>3</sub>)<sub>3</sub>•6H<sub>2</sub>O, and 12.5 g Zr(NO<sub>3</sub>)<sub>4</sub>•5H<sub>2</sub>O were dissolved in deionized water and stirred at 40 °C in a water bath for 30 minutes to form solution B. Then potassium carbonate solution (1 Mol/L) was added to solution A and solution B drop by drop, until the pH of each solution reached 11. After aging for 2 hours, the solution was filtered using deionized water and dried at 120°C overnight. The dried sample was then calcined at 850 °C for 4 hours and used for characterization and catalytic performance evaluation.

### Characterization of Catalysts

The BET surface area, pore diameter, and pore volume were measured by N<sub>2</sub> adsorption–desorption at 77 K, using the BET analysis method with an Autosorb-1 Quantachrom BET surface area analyzer. The Powder XRD patterns of the catalysts were obtained with PANalytical X'Pert PRO X-ray diffractometer with a Cu K<sub>α</sub>(λ=0.15418 m). The diffraction angle 2θ ranged from 10° to 90° and the scan speed was 5° min<sup>-1</sup>. The photomultiplier tube voltage was 40 kV and tube current was 30 mA. The catalyst surface morphology was observed by scanning electron microscopy (SEM, FEI Model SIRION-100). Temperature-programmed reduction (TPR) was performed to determine the reduction behavior of CeO<sub>2</sub>, ZrO<sub>2</sub>, and the Ni species on the support. The catalysts were first heated at 250 °C with a N<sub>2</sub> flow of 30 mL/min for 30 minutes. Then it was cooled to room temperature and reheated to 900 °C at 10 °C/min. A flow rate of 30 mL/min of 10% H<sub>2</sub> in N<sub>2</sub> was used for the reduction. A thermal conductivity detector (TCD) was employed to determine the amount of hydrogen consumed.

### Catalytic Activity Measurements

Catalytic activity measurements were carried out in a fixed bed reactor (ϕ 8 mm quartz tube) under atmospheric pressure. 1 mL catalyst powder in the 40-60 mesh size range was placed in the middle of a quartz reactor and supported on quartz fiber. Prior to the reforming reaction, the temperature of catalyst layer in the reactor rose to 800°C, and the catalyst was reduced in 50mL/min hydrogen stream for 4 hours. The ethanol solution was fed into the reactor by a peristaltic pump, gasified at 150°C, and mixed with N<sub>2</sub> before flowing into the fixed bed reactor. The gas products of ethanol reforming were analyzed on-line by gas chromatography. Among them H<sub>2</sub>, N<sub>2</sub>, CO, and CO<sub>2</sub> were detected by thermal conductivity detector, while CH<sub>4</sub> and C<sub>2</sub>-C<sub>3</sub> gases were detected by hydrogen flame ionization detector.

Ethanol steam reforming was carried out at different temperatures (T), steam-to-carbon ratios (S/C), and carbon-equivalent space velocities (G<sub>C1</sub>HSV). According to equation (1), the H<sub>2</sub> selectivity and carbon conversion were calculated as follows:

$$\text{H}_2 \text{ Selectivity} = \frac{\text{mole of H}_2 \text{ obtained}}{3 * \text{mole of carbon in the feed}} * 100\% \quad (5)$$

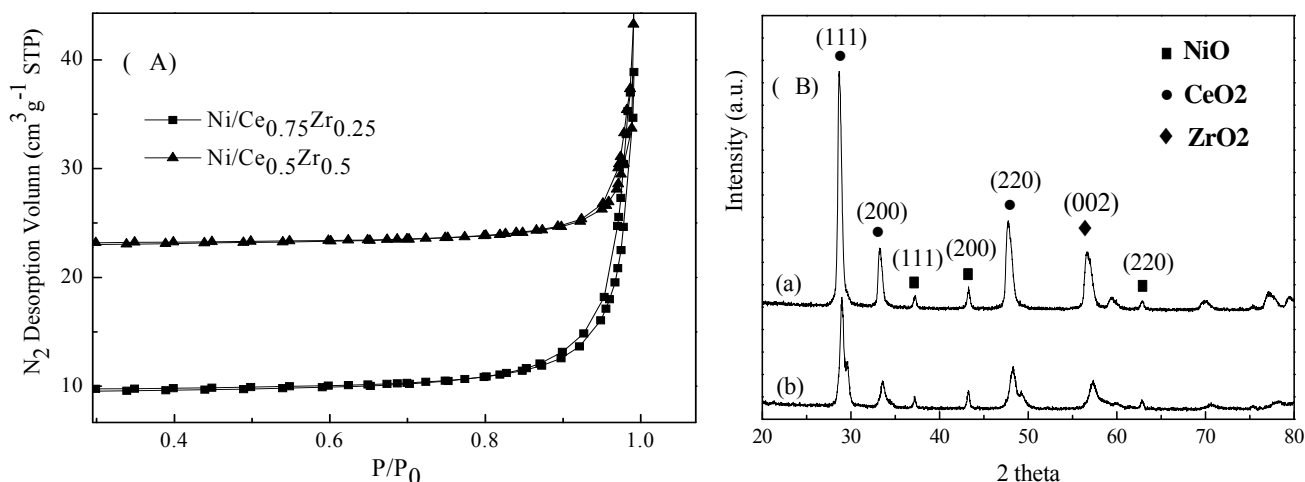
$$\text{Carbon Conversion \%} = \frac{\text{moles of carbon in (CO + CO}_2 + \text{CH}_4 + \text{C}_2 - 3) \text{ obtained}}{\text{moles of carbon in the feed}} * 100\% \quad (6)$$

## RESULTS AND DISCUSSION

### Catalyst Characterization

Figure 1(A) shows the N<sub>2</sub> adsorption-desorption isotherms of Ni/CeO<sub>2</sub>-ZrO<sub>2</sub>. The hysteresis loops were formed due to capillary condensation of N<sub>2</sub> molecules occurring in the pores of the catalysts. The pore diameters of catalysts Ni/Ce<sub>0.75</sub>Zr<sub>0.25</sub> and Ni/Ce<sub>0.5</sub>Zr<sub>0.5</sub> were either mesopores or macropores, since their hysteresis loops were located in the high-pressure area. The average pore diameters of the two catalysts were calculated using the BJH method. As shown in Table 1, the BET surface area and pore volume of Ni/Ce<sub>0.75</sub>Zr<sub>0.25</sub> were both larger than those of Ni/Ce<sub>0.5</sub>Zr<sub>0.5</sub>.

The XRD diffraction patterns of the catalysts are shown in Fig.1 (B). The two Ni/CeO<sub>2</sub>-ZrO<sub>2</sub> catalysts had almost the same diffraction peaks, which indicated that merely changing molar ratio of Ce/Zr within the given range did not generate new crystal structures. The peaks corresponding to NiO remained low even with 15wt %Ni, showing that NiO was present in the form of small particles and was well dispersed in the CeO<sub>2</sub>-ZrO<sub>2</sub> solid solution structure. The CeO<sub>2</sub> (111) peak intensity from the Ni/Ce<sub>0.75</sub>Zr<sub>0.25</sub> catalyst was higher than Ni/Ce<sub>0.5</sub>Zr<sub>0.5</sub> at 2θ = 28.65° due to the higher content of Ce. The CeO<sub>2</sub> (111) peak from the Ni/Ce<sub>0.5</sub>Zr<sub>0.5</sub> XRD pattern was wider than from Ni/Ce<sub>0.75</sub>Zr<sub>0.25</sub>, which was possibly caused by the smaller crystal size or lattice distortion.

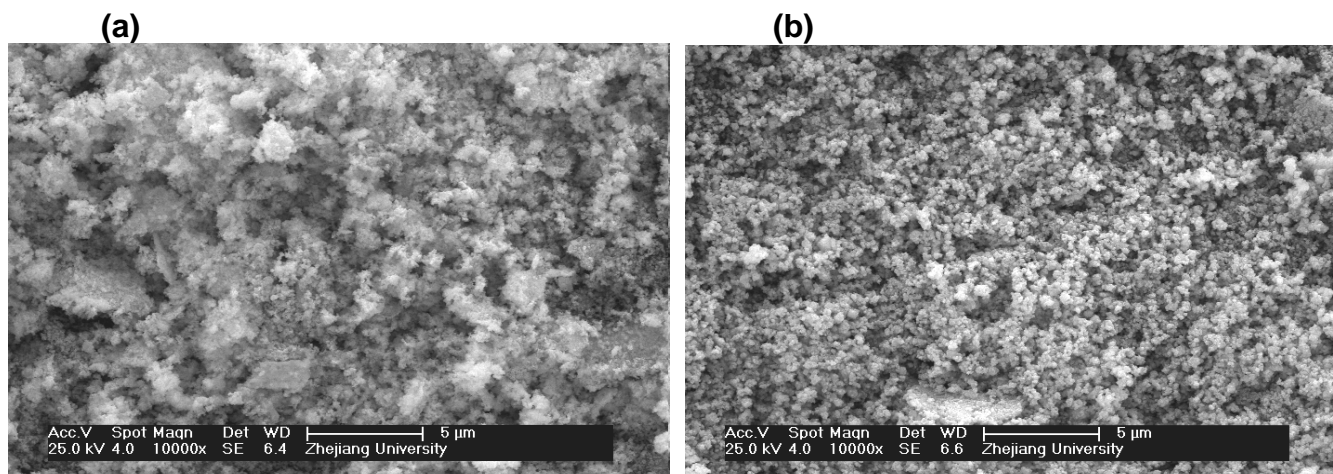
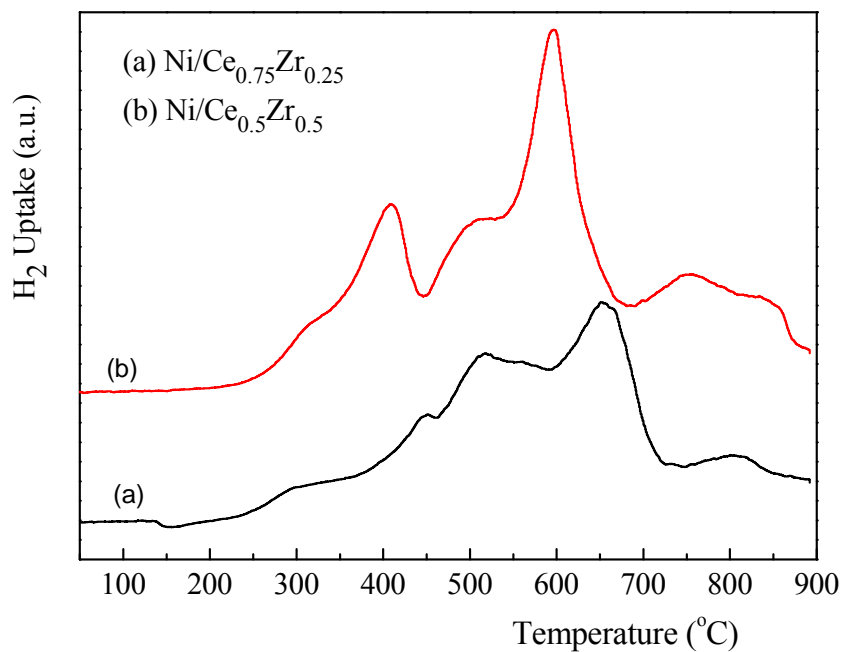


**Fig. 1.** Catalysts characterization: (A) N<sub>2</sub> adsorption-desorption isotherms; (B) XRD of Ni/CeO<sub>2</sub>-ZrO<sub>2</sub>: (a) Ni/Ce<sub>0.75</sub>Zr<sub>0.25</sub>; (b) Ni/Ce<sub>0.5</sub>Zr<sub>0.5</sub>

**Table 1.** Textural Property of Ni/CeO<sub>2</sub>-ZrO<sub>2</sub> Catalysts

Catalysts	A <sub>BET</sub> (m <sup>2</sup> /g)	V <sub>p</sub> (cm <sup>3</sup> /g)	D <sub>p</sub> (nm)
Ni/Ce <sub>0.75</sub> Zr <sub>0.25</sub>	5.9	0.05	43.1
Ni/Ce <sub>0.5</sub> Zr <sub>0.5</sub>	4.0	0.04	66.0

Figure 2 presents SEM images of the two catalysts. It can be seen that the surface of the two Ni/CeO<sub>2</sub>-ZrO<sub>2</sub> catalysts both had a continuous and uniform appearance. The particle size varied as the molar ratio of Ce/Zr changed from 0.75/0.25 to 0.5/0.5.

**Fig. 2.** SEM of Ni/CeO<sub>2</sub>-ZrO<sub>2</sub>: (a) Ni/Ce<sub>0.75</sub>Zr<sub>0.25</sub>; (b) Ni/Ce<sub>0.5</sub>Zr<sub>0.5</sub>**Fig. 3.** TPR profiles of Ni/Ce-Zr catalysts: (a) Ni/Ce<sub>0.75</sub>Zr<sub>0.25</sub>, (b) Ni/Ce<sub>0.5</sub>Zr<sub>0.5</sub>

TPR profiles of fresh Ni/Ce-Zr catalysts are given in Fig. 3. This shows the reduction peaks of NiO and CeO<sub>2</sub>-ZrO<sub>2</sub>. Two CeO<sub>2</sub> peaks were evident in the profiles of both catalysts, including a low-temperature peak and a high-temperature peak, due to the reduction of the surface layer of CeO<sub>2</sub> and the reduction of bulk oxygen (Trovarelli et al.1997). The CeO<sub>2</sub> peaks of catalyst Ni/Ce<sub>0.75</sub>Zr<sub>0.25</sub> were at 515°C and at 650°C, and those of catalyst Ni/Ce<sub>0.5</sub>Zr<sub>0.5</sub> were at 500 °C and 600 °C. The ZrO<sub>2</sub> did not show any reduction peak in this range of temperature according to Biswas (2007), but the presence of ZrO<sub>2</sub> can greatly influence the reduction temperature of CeO<sub>2</sub>. The reduction peak of NiO in catalyst Ni/Ce<sub>0.75</sub>Zr<sub>0.25</sub> was at 450 °C, while the reduction temperature decreased to 400 °C in the plot for Ni/Ce<sub>0.5</sub>Zr<sub>0.5</sub>, indicating that the different ratio of Ce/Zr has a significant effect on the reduction temperature of NiO. The wide temperature ranges of the peaks indicate a broad particle size distribution.

### Catalytic Performance

In our experiments, the catalytic performance of Ni/CeO<sub>2</sub>-ZrO<sub>2</sub> catalysts was evaluated based on the ethanol steam reforming reaction in a fixed bed reactor. The composition of the gas products, H<sub>2</sub> selectivity, and carbon conversion over Ni/CeO<sub>2</sub>-ZrO<sub>2</sub> catalysts were investigated.

#### Measurement of Catalyst Stability

The catalyst stability was tested at T=725 °C, S/C=9.2 and G<sub>C1</sub>SHV=345 h<sup>-1</sup> for 600 minutes, giving the data shown in Fig. 4. The stability data for catalyst Ni/Ce<sub>0.75</sub>Zr<sub>0.25</sub> in Fig. 4(a) indicates that its catalytic activity did not decline noticeably over 600 minutes. The concentration of CH<sub>4</sub> was zero in Fig. 4(a) and Fig. 4(b), which means that both catalysts Ni/Ce<sub>0.75</sub>Zr<sub>0.25</sub> and Ni/Ce<sub>0.5</sub>Zr<sub>0.5</sub> performed very well in reforming CH<sub>4</sub>.

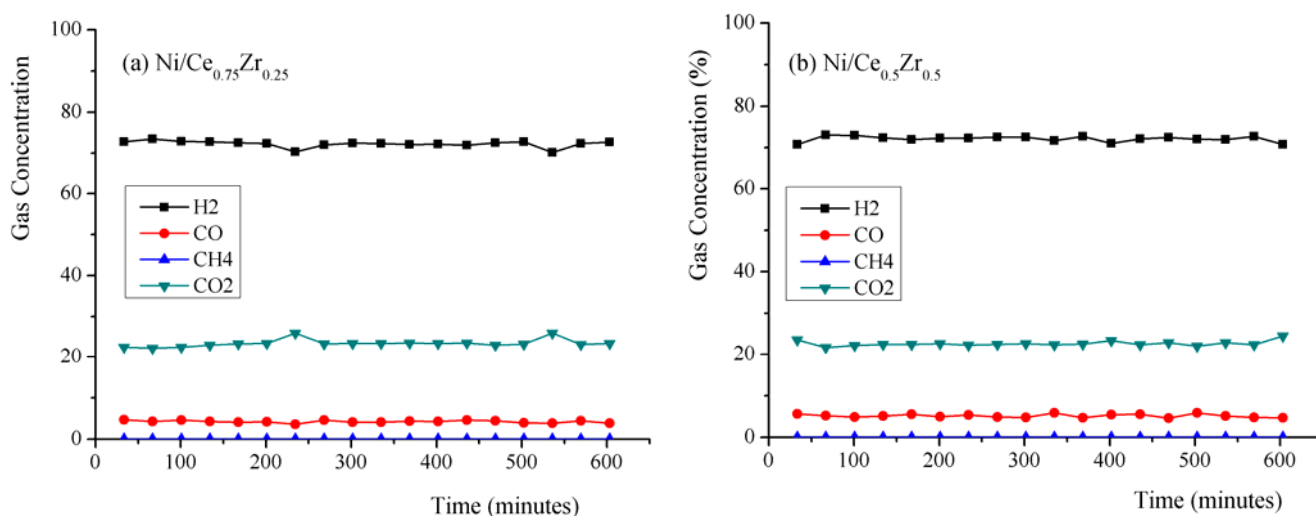
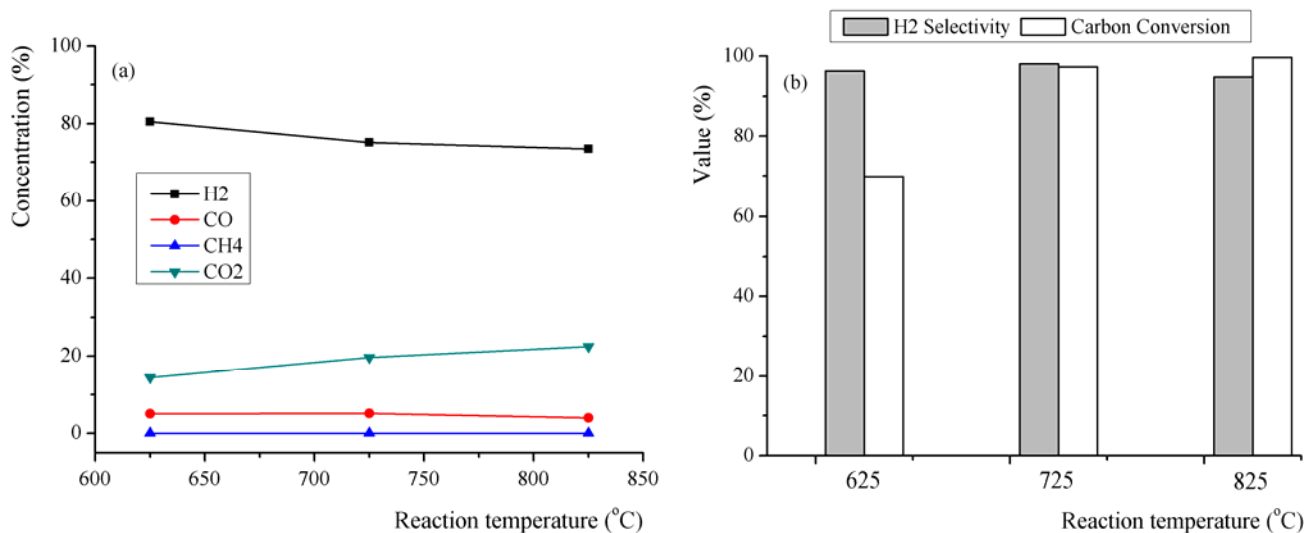
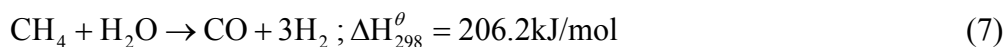


Fig. 4. Test of catalyst stability

### Effects of temperature

The effects of temperature on the ESR process at  $G_{C1}HSV=345 \text{ h}^{-1}$  and  $S/C=9.2$  over  $Ni/Ce_{0.75}Zr_{0.25}$  catalyst were evaluated. Figure 5 shows that the molar concentrations of CO, CH<sub>4</sub>, CO<sub>2</sub>, and H<sub>2</sub> did not show much fluctuation as the temperature increased. H<sub>2</sub> selectivities of over 90% were obtained at 625 °C, 725 °C, and 825 °C. The H<sub>2</sub> selectivity reached a maximum value of 98.1% at  $T=725 \text{ °C}$ , and the carbon conversion reached 100% at  $T=825 \text{ °C}$ , meaning that nearly all of the ethanol was converted during the reforming process.  $T=725 \text{ °C}$  was more appropriate for ethanol steam reforming over  $Ni/Ce_{0.75}Zr_{0.25}$ .

Figure 5 (a) shows that the CH<sub>4</sub> content in the gas products was close to zero, meaning that the catalyst performed well for the catalytic conversion of methane. Methane was transformed into CO and H<sub>2</sub> through the methane steam reforming reaction (Eq. (7)) and the CO<sub>2</sub> reforming reaction (Eq. (8)), which further increased the selectivity of hydrogen. The methane steam reforming over the Ni/Ce-Zr catalysts has been investigated by Laosiripojana (2005), who observed good methane steam reforming performance. The performance of Ni/Ce-Zr catalysts in methane reforming with CO<sub>2</sub> was also investigated by Montoya (2000) and Horváth (2011), where a methane conversion of 98% was obtained. The results from our experiments are therefore consistent with the literatures.



**Fig. 5.** Effects of reaction temperatures for  $Ni/Ce_{0.75}Zr_{0.25}$  at  $G_{C1}HSV=345 \text{ h}^{-1}$  and  $S/C=9.2$ : (a) Concentrations of gas products; (b) H<sub>2</sub> selectivity and carbon conversion

### Effects of $G_{C1HSV}$

Figure 6 shows the composition of gas products,  $H_2$  selectivity, and carbon conversion for  $T=725\text{ }^\circ\text{C}$  and  $S/C=9.2$ . The concentration of CO,  $CH_4$ ,  $CO_2$ , and  $H_2$  changed little with the increase of  $G_{C1HSV}$ , while the  $H_2$  yield and carbon conversion declined. The highest  $H_2$  selectivity was at  $345\text{ h}^{-1}$  and tended to fall as the  $G_{C1HSV}$  increased. This is mainly because the real reaction time inside the catalyst layer was reduced as the  $G_{C1HSV}$  increased from  $345$  to  $1725\text{ h}^{-1}$ , and some reactants were unable to react sufficiently before they left. This phenomenon has also been mentioned elsewhere (Deng 2008). The  $H_2$  selectivity increased to some extent when  $G_{C1HSV}$  was  $1725\text{ h}^{-1}$ , which was possibly caused by the improvement of heat and mass transfer conditions. However,  $G_{C1HSV}$  of  $345\text{ h}^{-1}$  still produced higher hydrogen selectivity.

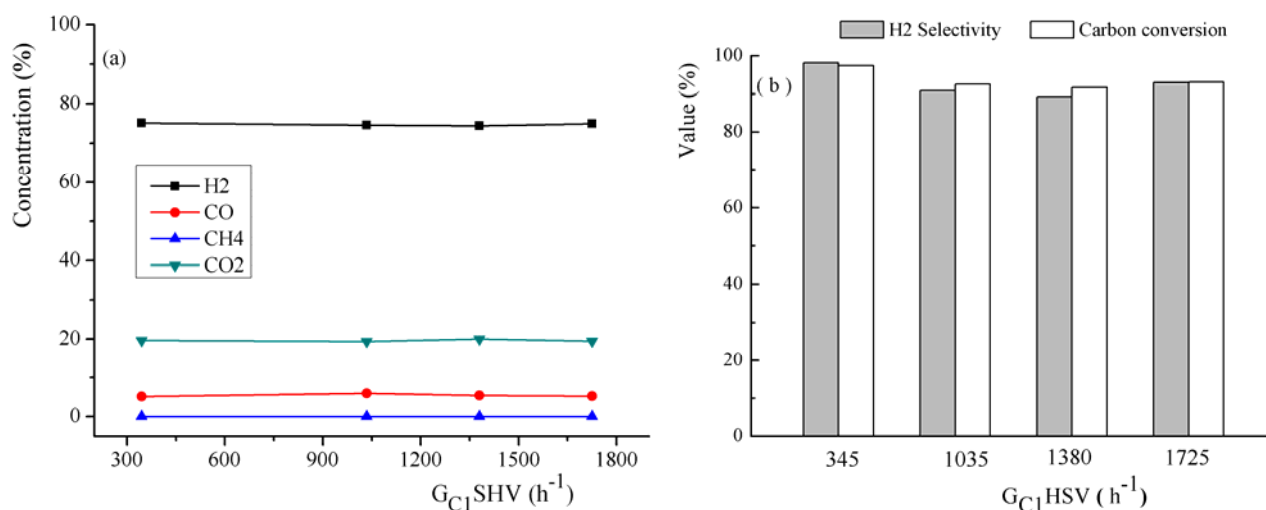


**Fig. 6.** Effects of  $G_{C1HSV}$  for  $Ni/Ce_{0.75}Zr_{0.25}$  at  $T=725\text{ }^\circ\text{C}$  and  $S/C=9.2$ :  
(a) Concentrations of gas products. (b)  $H_2$  selectivity and carbon conversion

### Performance comparison under different $S/C$

The performances of  $Ni/Ce_{0.75}Zr_{0.25}$  and  $Ni/Ce_{0.5}Zr_{0.5}$  were compared for different  $S/C$  ratios at  $T=725\text{ }^\circ\text{C}$  and  $G_{C1HSV}=345\text{ h}^{-1}$  (Fig. 7). For  $Ni/Ce_{0.75}Zr_{0.25}$ , the  $H_2$  selectivity increased from 47.2 % to 98.1 % when the  $S/C$  ratio changed from 2.5 to 9.2. This phenomenon may be well explained by Eq. (1) and Eq. (3). As the concentration of water in the feed increases, the equilibrium of the ESR reforming reaction (Eq. (1)) and WGS reaction (Eq. (3)) favors the right hand side of the equation, which results in an increase of hydrogen selectivity.

Comparing Fig. 7(a) with Fig. 7(b), the  $Ni/Ce_{0.75}Zr_{0.25}$  catalyst showed a higher carbon conversion than  $Ni/Ce_{0.5}Zr_{0.5}$  catalyst. This was in agreement with the results of other researchers (Biswas et al. 2007). It is clear that support plays a significant role for  $Ni/CeO_2$ - $ZrO_2$  catalysts in the steam reforming reaction. It has been reported that a higher  $CeO_2$  molar ratio favored the cubic face of ceria-zirconia, which has better activity for redox coupling between  $Ce^{3+}$  and  $Ce^{4+}$  (Hori et al. 1998). A higher molar ratio in the solid solution of Ce-Zr also improves the conversion of ethanol.

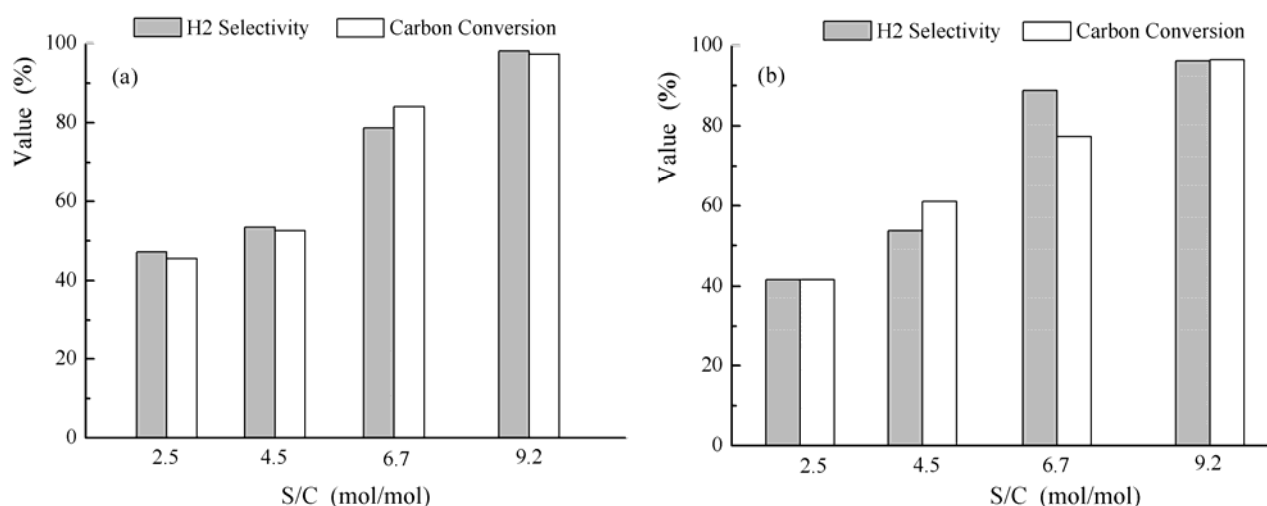


**Fig. 7.** Performances on H<sub>2</sub> selectivity and carbon conversion  
(a) Ni/Ce<sub>0.75</sub>Zr<sub>0.25</sub>; (b) Ni/Ce<sub>0.5</sub>Zr<sub>0.5</sub>

## CONCLUSIONS

1. The self-prepared Ni/CeO<sub>2</sub>-ZrO<sub>2</sub> catalysts performed well in the ethanol steam reforming reaction for hydrogen production. The highest H<sub>2</sub> selectivity of 98.1% was obtained with  $G_{C1}HSV=345h^{-1}$  and S/C=9.2 over the Ni/Ce<sub>0.75</sub>Zr<sub>0.25</sub> catalyst at T=725 °C, while the highest carbon conversion of 100% was obtained at T=825 °C.
2. The catalytic performance of Ni/Ce<sub>0.75</sub>Zr<sub>0.25</sub> was slightly better than Ni/Ce<sub>0.5</sub>Zr<sub>0.5</sub> under the same conditions, which indicated that the molar ratio of Ce to Zr affected the ethanol reforming reaction.
3. Temperature (T), carbon-equivalent space velocity ( $G_{C1}HSV$ ), and S/C all had effects on the ethanol reforming. When the temperature and space velocity were kept constant, higher hydrogen selectivity and carbon conversion were obtained as the value of S/C increased.

## ACKNOWLEDGMENTS

The authors are grateful for financial support from the National High Technology Research and Development Program of China (2009AA05Z407), the International Science and Technology Cooperation Program (2009DFA61050), the Research Fund for the Doctoral Program of Higher Education of China (20090101110034), the National Science & Technology Pillar Special Program (2011BAD22B06), the Zhejiang Provincial Natural Science Foundation of China (R1110089), and the Zhejiang Provincial Key Science and Technology Innovation Team (2009R50012)

## REFERENCES CITED

- Akande, A. J., Idem, R. O., and Dalai, A. K. (2005). "Synthesis, characterization and performance evaluation of Ni/Al<sub>2</sub>O<sub>3</sub> catalysts for reforming of crude ethanol for hydrogen production," *Applied Catalysis A - General* 287(2), 159-175.
- Biswas, P., and Kunzru, D. (2007). "Steam reforming of ethanol for production of hydrogen over Ni/CeO<sub>2</sub>-ZrO<sub>2</sub> catalyst: Effect of support and metal loading," *International Journal of Hydrogen Energy* 32(8), 969-980.
- Breen, J. P., Burch, R., and Coleman, H. M. (2002). "Metal-catalyzed steam reforming of ethanol in the production of hydrogen for fuel cell applications," *Applied Catalysis B: Environmental* 39(1), 65-74.
- Chen, Y. Z., Shao, Z. P., and Xu, N. P. (2008). "Ethanol steam reforming over Pt catalysts supported on Ce<sub>x</sub>Zr<sub>1-x</sub>O<sub>2</sub> prepared via a glycine nitrate process," *Energy & Fuels* 22(3), 1873-1879.
- Czernik, S., French, R., Feik, C., and Chornet, E. (2002). "Hydrogen by catalytic steam reforming of liquid byproducts from biomass thermoconversion processes," *Industrial & Engineering Chemistry Research* 41(17), 4209-4215.
- Deng, X., Sun, J., Yu, S., Xi, J., Zhu, W., and Qiu, X. (2008). "Steam reforming of ethanol for hydrogen production over NiO/ZnO/ZrO<sub>2</sub> catalysts." *INTERNATIONAL JOURNAL OF HYDROGEN ENERGY*, 33(3), 1008-1013.
- Fishtik, I., Alexander, A., Datta, R., and Geana, D. (2000). "A thermodynamic analysis of hydrogen production by steam reforming of ethanol via response reactions," *International Journal of Hydrogen Energy* 25(1), 31-45.
- Horváth, A., Stefler, G., Geszti, O., Kienneman, A., Pietraszek, A., and Gucci, L. (2011). "Methane dry reforming with CO<sub>2</sub> on CeZr-oxide supported Ni, NiRh and NiCo catalysts prepared by sol-gel technique: Relationship between activity and coke formation." *Catalysis Today* 169(1), 102-111
- Hori, C. E., Permana, H., Ng, K. Y. S., Brenner, A., More, K., Rahmoeller, K. M., and Belton, D. (1998). "Thermal stability of oxygen storage properties in a mixed CeO<sub>2</sub>-ZrO<sub>2</sub> system," *Applied Catalysis B - Environmental* 16(2), 105-117.
- Laosiripojana, N., and Assabumrungrat, S. (2005). "Methane steam reforming over Ni/Ce-ZrO<sub>2</sub> catalyst: Influences of Ce-ZrO<sub>2</sub> support on reactivity, resistance toward carbon formation, and intrinsic reaction kinetics." *Applied Catalysis A: General*, 290(1-2), 200-211.
- Liguras, D. K., Kondarides, D. I., and Verykios, X. E. (2003). "Production of hydrogen for fuel cells by steam reforming of ethanol over supported noble metal catalysts," *Applied Catalysis B - Environmental* 43(4), 345-354.
- Luckow, P., Wise, M. A., Dooley, J. J., and Kim, S. H. (2010). "Large-scale utilization of biomass energy and carbon dioxide capture and storage in the transport and electricity sectors under stringent CO<sub>2</sub> concentration limit scenarios," *International Journal of Greenhouse Gas Control* 4(5), 865-877.
- Marino, F., Baronetti, G., Jobbagy, M., and Laborde, M. (2003). "Cu-Ni-K/gamma-Al<sub>2</sub>O<sub>3</sub> supported catalysts for ethanol steam reforming formation of hydroxalcalite-type compounds as a result of metal-support interaction," *Applied Catalysis A - General* 238(1), 41-54.

- Montoya, J. A., Romero-Pascual, E., Gimon, C., Angel, P. D., and Monzón, A. (2000). "Methane reforming with CO<sub>2</sub> over Ni/ZrO<sub>2</sub>-CeO<sub>2</sub> catalysts prepared by sol-gel." *Catalysis Today*, 63(1), 71-85.
- Silva, A. M. d., Souza, K. R. d., Jacobs, G., Graham, U. M., Davis, B. H., Mattos, L. V., and Noronha, F. B. (2011). "Steam and CO<sub>2</sub> reforming of ethanol over Rh/CeO<sub>2</sub> catalyst," *Applied Catalysis B: Environmental* 102(1), 94-109.
- Song, C. (2005). "Overview of hydrogen production options for developing hydrogen energy," *Journal of Fuel Chemistry and Technology* 33(6), 641-649.
- Trovarelli, A., Zamar, F., Llorca, J., DeLeitenburg, C., Dolcetti, G., and Kiss, J. (1997). "Nanophase fluorite-structured CeO<sub>2</sub>-ZrO<sub>2</sub> catalysts prepared by high-energy mechanical milling - Analysis of low-temperature redox activity and oxygen storage capacity " *JOURNAL OF CATALYSIS* 169(2), 490-502.
- Tsisun, Y. L., Litvin, Y. F., Nefedov, B. K., and Stoyakina, K. I. (1981). "Liquid-phase hydrogenation of aromatic-hydrocarbons on a Ru/Al<sub>2</sub>O<sub>3</sub> catalyst," *Petroleum Chemistry* 21(2), 73-77.
- Vargas, J. C., Libs, S., Roger, A. C., and Kiennemann, A. (2005). "Study of Ce-Zr-Co fluorite-type oxide as catalysts for hydrogen production by steam reforming of bioethanol," *Catalysis Today* 107(8), 417-425.
- Wang, D., Montane, D., and Chornet, E. (1996). "Catalytic steam reforming of biomass-derived oxygenates: Acetic acid and hydroxyacetaldehyde," *Applied Catalysis A - General* 143(2), 245-270.
- Wang, H., Brady, M. P., More, K. L., Meyer, H. M., and Turner, J. A. (2004). "Thermally nitrated stainless steels for polymer electrolyte membrane fuel cell bipolar plates - Part 2: Beneficial modification of passive layer on AISI446," *J. Power Sources* 138(1-2), 79-85.

Article submitted: June 10, 2011; Peer review completed: July 23, 2011; Revised version received and accepted: August 23, 2011; Published: August 27, 2011.